Effects of Pluronic P85 on GLUT1 and MCT1 Transporters in the Blood-Brain Barrier

Elena V. Batrakova,[1] Yan Zhang,[1,4] Yili Li,[1] Shu Li,[1] Sergei V. Vinogradov,[1] Y. Persidsky,[2] Valery Yu. Alakhov,[3] Donald W. Miller,[1] and Alexander V. Kabanov[1,5]

Received February 13, 2004; accepted April 20, 2004

Purpose. The amphiphilic block copolymer Pluronic P85 (P85) increases the permeability of the blood-brain barrier (BBB) with respect to a broad spectrum of drugs by inhibiting the drug efflux transporter, P-glycoprotein (Pgp). In this regard, P85 serves as a promising component for CNS drug delivery systems. To assess the possible effects of P85 on other transport systems located in the brain, we examined P85 interactions with the glucose (GLUT1) and monocarboxylate (MCT1) transporters.

Methods. Polarized monolayers of primary cultured bovine brain microvessel endothelial cells (BBMEC) were used as an *in vitro* model of the BBB. ^{3}H-2-deoxy-glucose and ^{14}C-lactate were selected as GLUT1 and MCT1 substrates, respectively. The accumulation and flux of these substrates added to the luminal side of the BBMEC monolayers were determined.

Results. P85 has little effect on ^{3}H-2-deoxy-glucose transport. However, a significant decrease ^{14}C-lactate transport across BBMEC monolayers is observed. Histology, immunohistochemistry, and enzyme histochemistry studies show no evidence of P85 toxicity in liver, kidney, and brain in mice.

Conclusions. This study suggests that P85 formulations do not interfere with the transport of glucose. This is, probably, due to compensatory mechanisms in the BBB. Regarding the transport of monocarboxylates, P85 formulations might slightly affect their homeostasis in the brain, however, without any significant toxic effects.

KEY WORDS: blood-brain barrier; glucose; metabolism; monocarboxylates; Pluronic.

INTRODUCTION

The blood-brain barrier (BBB) restricts entry of diagnostic and therapeutic agents to the brain from the vasculator. The low permeability of the BBB is attributed to the brain microvessel endothelial cells, which form tight junctions and have low pinocytic activity (1,2). In addition, these cells express drug efflux transporters such as P-glycoprotein (Pgp), which actively extrudes drugs from the brain to the blood (3,4). Substrates for these transporters include analgetics (5), HIV proteases inhibitors (6), antibiotics (7), antiepileptics (8), and anti-inflammatory drugs (9).

Our previous studies have demonstrated that poly(ethylene oxide)-poly(propylene oxide) block copolymers (Pluronics) are potent inhibitors of the Pgp drug efflux system in the BBB (10). Specifically, formulation of Pgp-dependent drugs with Pluronic P85 (P85) results in significant increases in their transport to the brain (11). The inhibition of Pgp by P85 involves two effects: 1) decreasing affinity of Pgp with respect to both ATP and the drug molecules and 2) depletion of intracellular ATP in the brain microvessel endothelial cells. The synergy between these two effects results in the pronounced inhibition of Pgp drug efflux function. The purpose of the current study is to assess whether P85 affects other transport systems in the BBB. Two transporters that play a crucial role in the energy metabolism in the brain were chosen: GLUT1, a transporter of glucose, and MCT1, a transporter of monocarboxylates.

Using polarized monolayers of bovine brain microvessel endothelial cells (BBMEC) as an *in vitro* model of the BBB the effects of P85 on the accumulation and flux of 2-deoxyglucose, a GLUT1 substrate, and lactate, an MCT1 substrate were examined. The results suggest that the block copolymer has little, if any, effect on the glucose supply to the brain, and decreases the flux of lactate across the BBMEC monolayers. The inhibition of the lactate transporter may be a consideration for the potential adverse effect of P85 in the central nervous system (CNS), which was addressed in toxicological studies in this paper.

MATERIALS AND METHODS

P85 Solutions

P85 was kindly provided by BASF Corp. (Parispany, NJ, USA). The molecular mass of the poly-oxypropylene (PO) segment in this sample was approximately 2500 and the content of poly-oxyethylene (EO) chains was approximately 50% (w/w). P85 was dissolved in assay buffer containing 150 mM NaCl, 25 mM $NaHCO_3$, 10 mM glucose, 10 mM HEPES, 3 mM KCl, 1.2 mM $MgSO_4$, 1.4 mM $CaCl_2$, and 0.4 mM K_2HPO_4, pH 7.4. ^{3}H-2-deoxy-glucose (^{3}H-2-DG) and ^{14}C-lactate (^{14}C-La) obtained from American Radiolabeled Chemicals, Inc. (St Louis, MO, USA) were added to the copolymer solutions and incubated at 37°C for at least 1 h prior to the subsequent use. No glucose was added to the assay buffer for the ^{3}H-2-DG studies.

Cell Isolation and Culture

BBMEC were isolated from fresh cow brains using a combination of enzymatic digestion and density centrifugation as described previously (12). The cells were maintained in MEM:F12 culture medium supplemented with 10% horse serum, heparin sulfate (100 μg/ml), amphotericin B (2.5 μg/ml), and gentamicin (50 μg/ml). All tissue culture media were

[1] College of Pharmacy, Department of Pharmaceutical Sciences, Nebraska Medical Center, Omaha, Nebraska 68198, USA.
[2] Center for Neurovirology and Neurodegenerative Disorders, and Departments of Pathology and Microbiology, Nebraska Medical Center, Omaha, Nebraska 68198, USA.
[3] Supratek Pharma Inc., Laval, PQ, Canada H7N 4Z3.
[4] Current address: Pfizer Global Research and Development, Ann Arbor, Michigan 48105, USA.
[5] To whom correspondence should be addressed. (e-mail: akabanov@unmc.edu)

ABBREVIATIONS: BBB, blood-brain barrier; BBMEC, bovine brain microvessel endothelial cells; CNS, central nervous system; CMC, critical micelle concentration; ^{14}C-La, ^{14}C-lactate**;** GLUT1, glucose transporter; ^{3}H-2-DG, ^{3}H-2-deoxyglucose; MCT1, monocarboxylate transporter; MDR, multidrug resistance; MRP, multidrug resistance–associated protein; Pgp, P-glycoprotein; P85, Pluronic P85.

obtained from Gibco Life Technologies, Inc. (Grand Island, NY, USA). Isolated BBMEC were seeded at a density of 50,000 cells/cm^2 in 24-well plates or 250,000 cells per insert (Transwell, Costar brand Tissue Culture products, Contd., Vernon Hills, IL, USA), and were used for accumulation or flux studies after reaching confluency (typically within 14 days).

Western Blot Analysis

The expression levels of GLUT1 and MCT1 in BBMEC was evaluated by immunobloting technique described previously (13). The monoclonal antibodies to GLUT1, sc-1605 (Santa Cruz Biotechnology, Santa Cruz, CA, USA), and to MCT1, AB3540P (Chemicon International, Temecula, CA, USA) were used at 1:100 dilutions. The monoclonal antibodies to β-actin, anti-β-1-chicken Integrin (Sigma Corp., St. Louis, MO, USA), were used at 1:200 dilution. The secondary horseradish peroxide-conjugated anti-mouse Ig antibodies (Amersham Life Sciences, Cleveland, OH, USA) were used at 1:1500 dilution. The specific protein bands were visualized using a chemiluminescence kit (Pierce, Rockford, IL, USA). The expression levels of GLUT1 and MCT1 were quantitated by densitometry (Nucleo Vision, Nucleo Tech, Curitiba-Pr., Brazil) and normalized to the constitutively expressed β-actin.

^{3}H-2-DG and ^{14}C-La Accumulation Studies

Effect of various concentrations of P85 on ^{3}H-2-DG and ^{14}C-La accumulation in the BBMEC was evaluated as described earlier (14). Briefly, confluent cell monolayers were pretreated with the assay buffer or solutions of P85 for 30 min at 37°C, and then incubated with ^{3}H-2-DG (specific activity 10 Ci/mmol, 1μCi/ml, 100 nM) or ^{14}C-La (specific activity 55 Ci/mmol, 1μCi/ml, 550 nM) in the assay buffer or P85 solutions for various time intervals (up to 2 h). After that, cells were washed with ice-cold PBS and solubilized in 1% Triton X-100 for subsequent determination of radioactivity (Tricarb 4000, Packard, Meriden, CT, USA). To confirm specificity of ^{3}H-2-DG and ^{14}C-La transport, effects of nonlabeled D- and L-glucose, as well as L-lactate were studied in BBMEC monolayers. All experiments were conducted in quadruplicate. The cellular accumulations of the solutes were normalized for the cellular protein content determined by Pierce BCA method (15).

Effects of P85 on Kinetic Parameters of ^{3}H-2-DG Transport

Effects of P85 on kinetic parameters of ^{3}H-2-DG transport were evaluated in homologous competition experiments with nonlabeled D-glucose using the radioligand saturation binding method (16). This method is the most effective one at minimizing the amount of radioligand needed in cases with high K_m values, such as GLUT1. For this purpose, the accumulation of ^{3}H-2-DG (100 nM) was assayed in the presence of increasing concentrations of nonlabeled 2-DG in assay buffer or in 1%wt P85 solution following the 15 min treatment. The data obtained from the inhibition experiments were converted to a saturation curve by the dilution factor (16). The maximal reaction rate (V_{max}) and apparent Michaelis constants (K_m) were determined from the obtained saturation curves (17). The entire curve fitting was carried out using GraphPad Prism 3.0 (GraphPad software, San Diego, CA, USA).

^{3}H-2-DG and ^{14}C-La Flux Studies

BBMEC permeability studies were carried out as previously described (14). Briefly, polycarbonate membrane inserts with confluent BBMEC monolayers were placed in Side-Bi-Side diffusion chambers (Crown Bio Scientific, Inc., Somerville, NJ, USA) and maintained at 37°C. The transepithelial electrical resistance (TEER) of the confluent BBMEC monolayers was ca. 165.0 ± 15.7 Ω · cm^2. First, the cell monolayers were pre-treated with the substrate-free assay buffer or P85 solutions (0.001–1%wt), and then, transport of ^{3}H-2-DG (100 nM) or ^{14}C-La (550 nM) in either assay buffer alone or in the corresponding P85 solution added to the luminal side of the monolayers was monitored by appearance of the radioactivity (Tricarb 4000, Packard, Meriden, CT, USA) in the receiver chamber on the abluminal side of the monolayers. All transport experiments were conducted in triplicate.

Quantitative Determination of Lactate in Extracellular Media

Confluent BBMEC monolayers were treated with various concentrations of P85 for 2 h at 37°C. Then, extracellular media was collected and centrifuged (10 min, 1500 rpm). Lactate in the supernatant was assayed using commercial kit (cat. no. 735-10, Sigma, St. Louis, MO, USA).

In Vivo Toxicity Evaluation of P85

To evaluate possible toxic effects of P85 *in vivo,* female C57/Bl/6 mice aged 11–12 weeks (Taconic Laboratories, Germantown, NY, USA) were injected three times i.v. with 1%wt P85 or physiologic saline solution (100 μl) via the tail vein (on 1st, 4th, and 7th day). On the 9th day, animals were sacrificed; liver, brain, and kidney were removed, washed in ice-cold saline, fixed in 4% phosphate-buffered paraformaldehyde, and paraffin embedded. Pathologic evaluation of the organs was performed on 5-μm paraffin sections stained with hematoxylin and eosin (H&E). To assess toxicity of the copolymer in the mice brain, enzyme histochemistry for adenosine triphosphatase (ATPase), expressed in endothelial cells was performed on frozen sections. ATPase was detected by insoluble deposits of calcium phosphate forming at the sites of ATPase expression. Cobalt chloride was exchanged for calcium to form cobalt phosphate at these sites with subsequent exposure to ammonium sulfide to generate a black insoluble precipitate. Sections were examined using a digital imaging system (MagnaFire digital camera) and software (Optronics, Goleta, CA, USA). The total area occupied by dye staining was quantified using Image-Pro Plus software (Media Cybernetics, Silver Spring, MD, USA) in 20 fields with a 20× objective, as previously described (18).

Mouse astrocytes were treated with polyclonal antibodies against glial fibrillary acid protein (GFAP) at 1:1000 dilution (Dako Corp., Carpinteria, CA, USA), and then, primary antibodies were detected by immunoperoxidase staining with 3,3′-diaminobenzidine as the chromogen (Vectastain Elite ABC kit, Vector Laboratories, Burlingame, CA, USA). All sections were counterstained with Mayer's hematoxylin. Deletion of the primary antibody or use of rabbit IgG (Dako

Corp.) served as controls. Immunostained tissues were analyzed using a Nikon Eclipse 800 microscope.

Statistical Analysis

All statistical tests were performed by GraphPad Prism 3.0 with two-way ANOVA and Newman-Keuls post-test for multiple comparisons. A minimum p value of 0.05 was estimated as the significance level for the all tests. The results are presented as means ± SEM.

RESULTS

Expression of GLUT1 and MCT1 in the BBMEC

Expression of GLUT1 and MCT1 in the BBMEC was validated by Western bloting analysis. As is seen in Fig. 1, the confluent BBMEC monolayers displayed significant amounts of both, GLUT1 and MCT1 proteins. These results confirm BBMEC monolayers as an *in vitro* model of the BBB and suitable for further studies of GLUT1 and MCT1 transporters.

Effects of P85 on GLUT1

Effects of P85 on ^{3}H-2-DG accumulation levels in the BBMEC were examined over the wide range of P85 concentrations (0.001–1% wt) (Fig. 2A). Subtle, but statistically significant increases in the ^{3}H-2-DG intracellular levels were observed in the presence of low concentrations of P85 (0.001–0.01% wt). By contrast, the exposure of the cells to high concentrations of the block copolymer (0.1–1% wt) resulted in significant decreases in ^{3}H-2-DG accumulation. The specificity of ^{3}H-2-DG transport mediated by GLUT1 was confirmed by experiments in which increasing amount of D-glucose were added to treatment solutions causing subsequent decreases in ^{3}H-2-DG intracellular concentrations (Fig. 2B). Addition of L-glucose had no effect on ^{3}H-2-DG accumulation (data not shown).

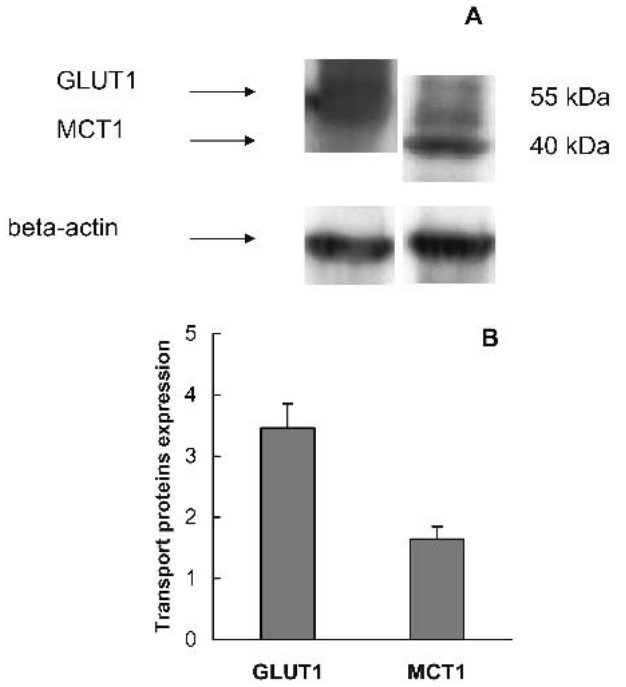

Fig. 1. (A) Western blot analysis of GLUT1 and MCT1 in the confluent BBMEC monolayers (for experimental conditions see "Materials and Methods"). The protein bands were visualized by chemoluminescence. (B) Levels of expression of the transport proteins normalized to β-actin.

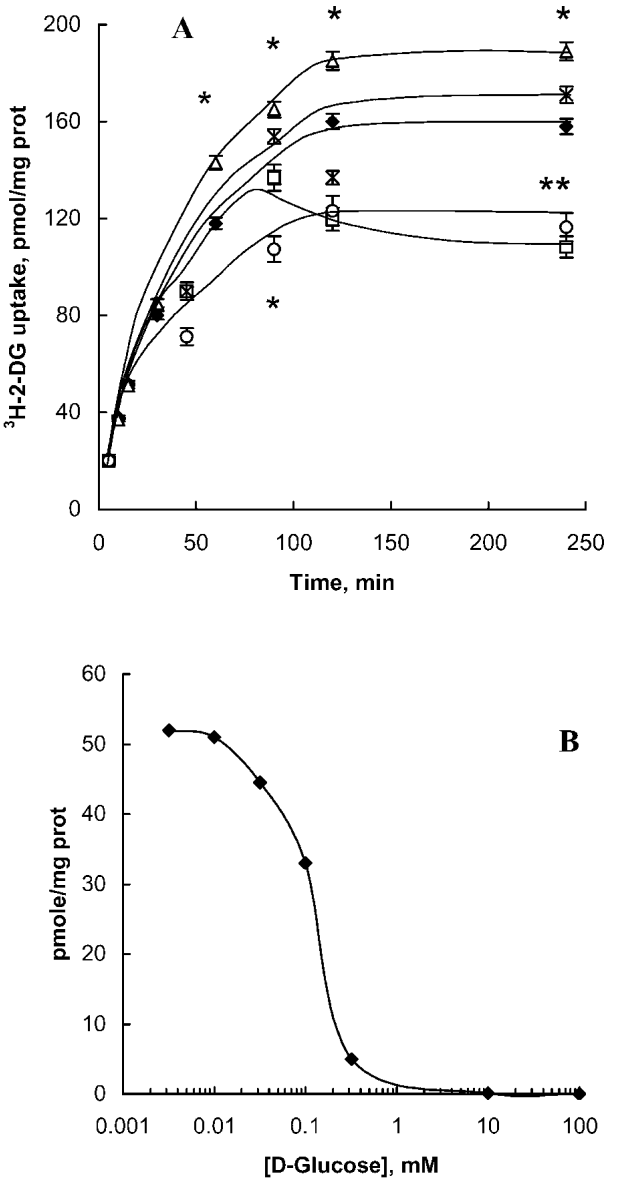

Fig. 2. (A) Effect of P85 on ^{3}H-2-DG accumulation in the BBMEC monolayers treated with solutions of 100 nM ^{3}H-2-DG in: assay buffer (filled diamonds); 0.001%wt P85 (crosses); 0.01%wt P85 (open triangles); 0.1%wt P85 (open squares); or 1%wt P85 (open circles). (B) Effect of D-glucose on accumulation of ^{3}H-2-DG in the BBMEC monolayers. All measurements were done at 15 min after addition of the substrate. Statistical significance of P85 effects compared to the P85-free controls is shown on the figure: (*) $p < 0.05$, (**) $p < 0.005$; $n = 4$.

The kinetic parameters of the glucose transport were determined using the radioligand saturation binding or the "cold saturation" method commonly used for substrates with high K_m values. For this experiment ^{3}H-2-DG was supplemented with increasing concentrations of unlabeled D-glucose, and

the accumulation of ^{3}H-2-DG was measured (Fig. 3). The maximal reaction rate (V_{max}) and apparent Michaelis constants (K_m), were determined as described in "Materials and Methods." V_{max} for GLUT1 in the absence of P85 is 2502.2 pmol mg^{-1} min^{-1}, and K_m is 0.079 mM. Treatment of the cells with 1% wt P85 slightly reduced V_{max} by 1.3 times (1927.2 pmol mg^{-1} min^{-1}) and increased K_m by approximately 1.8 times (0.1432 mM).

Figure 4 presents results of the flux studies of ^{3}H-2-DG across BBMEC monolayers exposed to the assay buffer, various concentrations of P85 (0.01%, 0.1%, 1% wt), and unlabeled D-glucose. The block copolymer had no effect on the flux of the substrate except for 0.01%wt. At this concentration P85 induced significant flux increases (by 40%) compared with the control group. Noteworthy, the flux of a paracellular marker, ^{3}H-mannitol, was not altered over the entire range of P85 concentrations confirming integrity of the monolayers (data not shown). Addition of D-glucose significantly reduced the flux of ^{3}H-2-DG (Fig. 4), thereby confirming specific GLUT1-mediated transport.

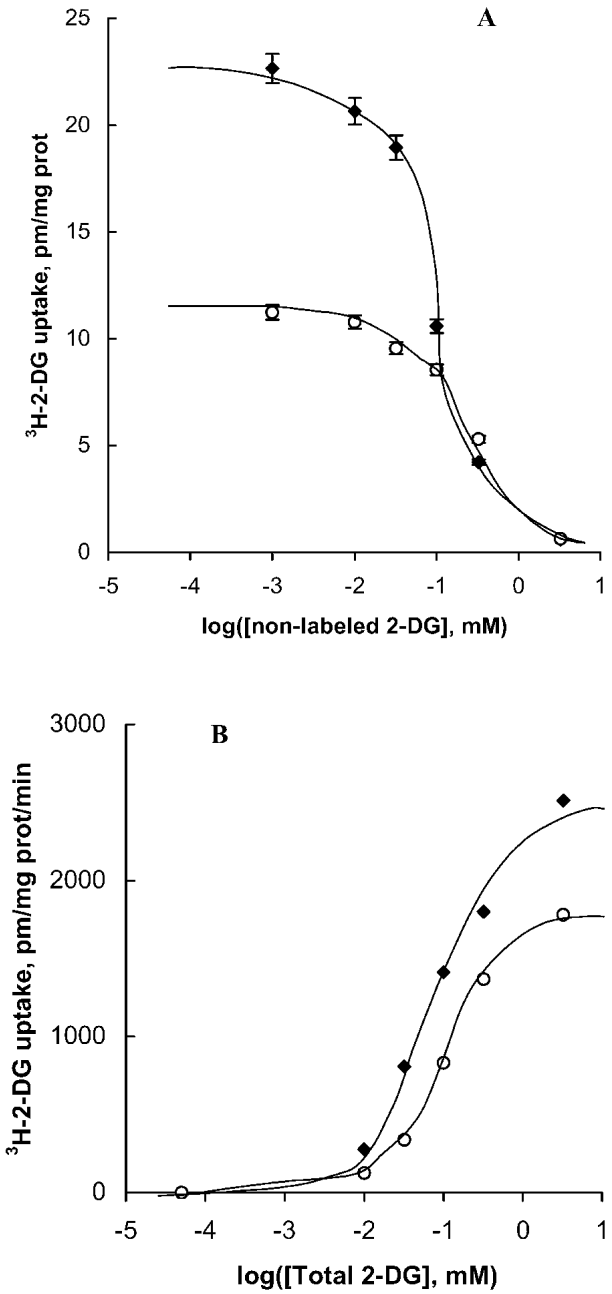

Fig. 3. Homologous inhibition experiments for 100 nM ^{3}H-2-DG accumulation in the presence of increasing concentrations of nonlabeled D-glucose in assay buffer (filled diamonds) or in 1%wt P85 (open circles); inhibition curve (A), and saturation curve (B).

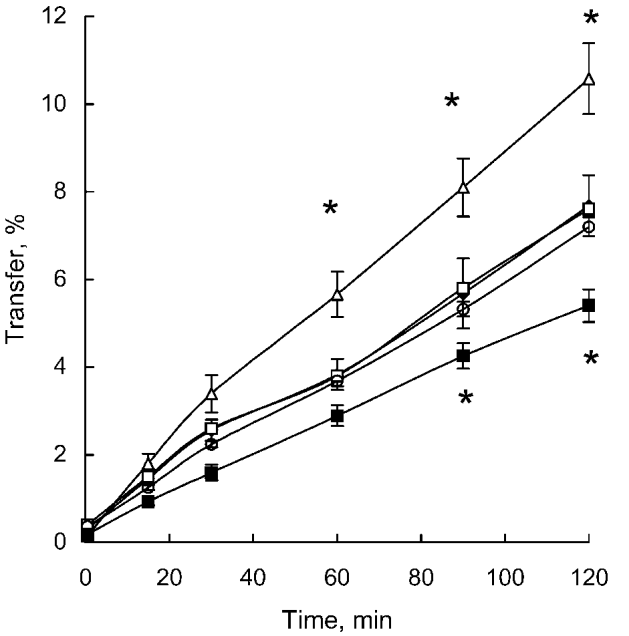

Fig. 4. Effect of P85 on ^{3}H-2-DG flux in the BBMEC monolayers. Transport of the probe from luminal to abluminal side was examined using the assay buffer (filled diamonds); 0.01%wt P85 (open triangles); 0.1%wt P85 (open squares); 1%wt P85 (open circles); or 10 mM of nonlabeled D-glucose (filled squares). Statistical significance of the P85 effects compared to the P85-free controls is shown on the figure: (*) $p < 0.05$, $n = 3$.

Effects of P85 on MCT1

^{14}C-La, a typical MCT1 substrate, displays unusual accumulation kinetics in BBMEC with an initial accumulation increase (at 15 min) followed by a decrease in the substrate intracellular accumulation levels (at 25–60 min) (Fig. 5A). Taking into account that ^{14}C-La can also be a substrate for organic anion efflux transporters (such as MRPs) we examined the uptake of ^{14}C-La in the presence of the MRPs inhibitor, indomethacin (10 μM), or with the MCT1 inhibitor, phloretin (50 μM). As is seen in the Fig. 5A, phloretin nearly completely abolished the 15-min maximum on the kinetics curve. By contrast, addition of indomethacin did not affect the maximal accumulation levels, although it did increase the accumulation of ^{14}C-La at later time points. Thus, the initial 15-min kinetic phase is likely to characterize the MCT1 function, while the subsequent phase corresponds to the substrate efflux. To validate this observation, we examined the effect of non-labeled lactate on the ^{14}C-La accumulation at the 15-min time point (Fig. 5B). Decreases in the ^{14}C-La accumulation levels in the presence of non-labeled lactate suggest specific MCT1-mediated transport.

The effects of P85 on ^{14}C-La accumulation in the

BBMEC were examined over a wide concentration range of the block copolymer (0.001–1%wt). Figure 6A shows the kinetics of ^{14}C-La accumulation, which are complicated by the effects of P85 on both MCT1 and MRPs transporters. To simplify analysis, we plotted the data for accumulation intracellular levels at only one 15-min time point over a range of P85 concentrations (Fig. 6A, insert**)**. As seen in the figure, P85 reduced ^{14}C-La intracellular levels with the greatest efficacy observed at 0.01%wt P85.

To confirm those results, we measured the amount of lactate remaining in the media following a 2-h exposure of BBMEC to various concentrations of P85 (Fig. 6B). Significant increases in the lactate levels in the extracellular media were observed with 0.01–1% wt P85, suggesting the inhibitory effect of the block copolymer on MCT1-mediated transport of lactate. Consistent with the results of the previous experiment, the greatest effect was observed at 0.01% wt P85.

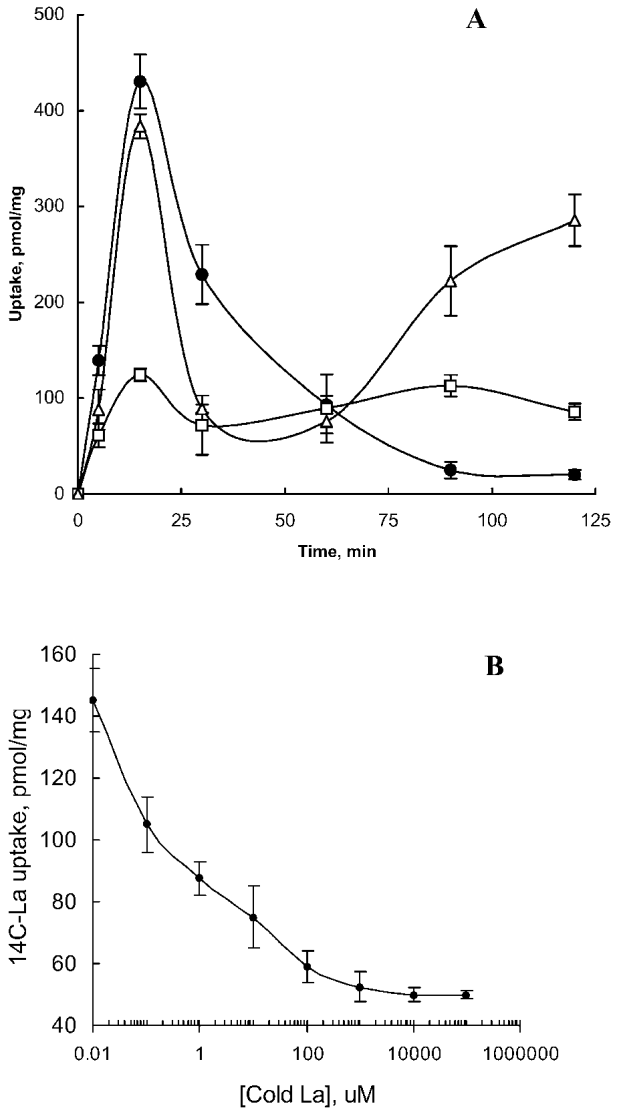

Fig. 5. (A) Kinetics of ^{14}C-La accumulation in the BBMEC monolayers. The cells were treated with 550 nM ^{14}C-La in: assay buffer (filled circles); 50μM phloretin (open squares); or 10 μM indomethacin (open triangles). (B) Saturation experiment with 550 nM ^{14}C-La and increased concentrations of nonlabeled L-lactate.

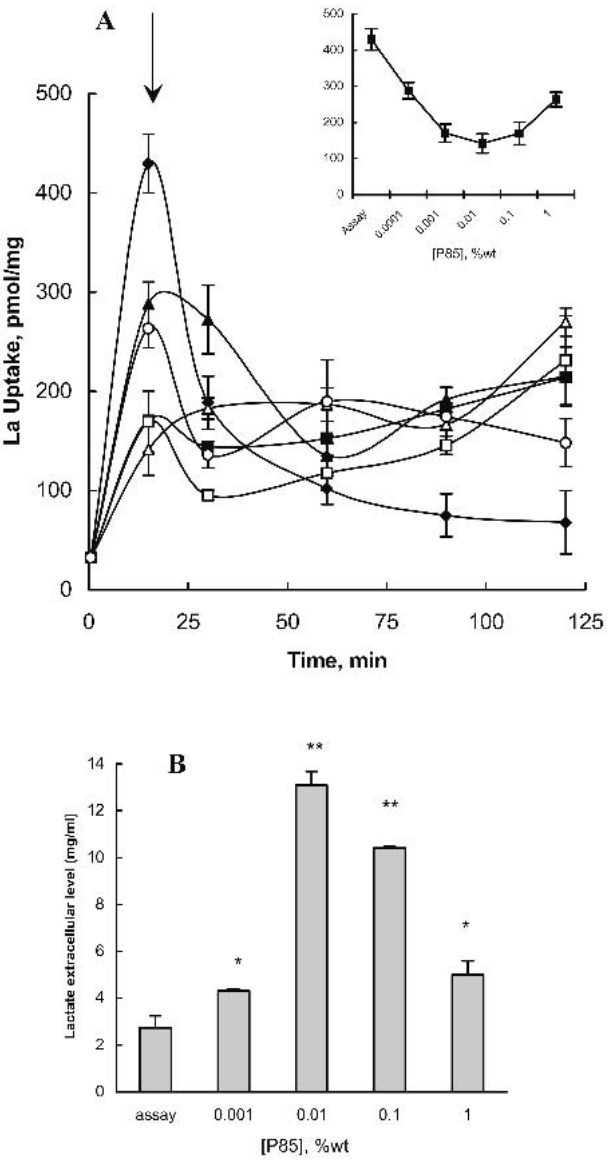

Fig. 6. (A) Effect of P85 on ^{14}C-La accumulation in the BBMEC monolayers. Accumulation of 550 nM ^{14}C-La was examined in: assay buffer (filled diamonds); 0.0001%wt P85 (filled triangles); 0.001%wt P85 (filled squares); 0.01%wt P85 (open triangles); 0.1%wt P85 (open squares); and 1%wt P85 (open circles). Inset: Intracellular accumulation levels of ^{14}C-La at the 15-min time point (indicated by the arrow). (B) lactate extracellular levels following 2-h treatment of BBMEC with various concentrations of P85. Statistical significance of the P85 effects compared to the P85-free controls is shown on the figure: (*) $p < 0.05$, (**) $p < 0.005$; $n = 4$.

Finally, we studied the transport of ^{14}C-La formulated with various concentrations of P85 across the BBMEC monolayers (Fig. 7). In agreement with the data obtained in the accumulation studies, the block copolymer decreased the transport of ^{14}C-La. The maximal inhibition effect was found at 0.01–0.1% wt P85, whereas at 1% wt P85 transport of ^{14}C-La was partially restored.

Histology, Immunohistochemistry, and Enzyme Histochemistry for Toxicological Evaluation of P85 Effects

To evaluate the potential toxic effects of P85 *in vivo*, mice were injected with 1% wt P85, the highest concentration

used, or with the physiologic solution as a control. Two days after the last injection, the animals were sacrificed, and the internal organs were collected at necropsy. Light microscopy of liver, kidney and brain was performed on hematoxylin and eosin (H&E)-stained paraffin sections. There was no evidence of nephrotoxicity, that is, acute tubular necrosis, glomerular changes or edema/fibrosis of interstitium in treated mice compared with controls (data not shown). Liver tissue from both controls and treated animals demonstrated absence of significant hepatocyte necrosis, micro- or macrosteatosis, inflammatory changes in bile ducts or microvessels (Figs. 8A and 8B). Light microscopie examination of brain tissue showed no evidence of neuronal injury, edema or brakedown of the BBB.

Next, we evaluated neuro-inflammatory responses (astrogliosis) and structural integrity of the BBB in mice treated with P85 or physiologic buffer. The level of astrogliosis as detected by GFAP staining was not altered in the treatment group compared with controls (Figs. 8B and 8E). We also assessed the activity of ATPase (detected *in situ* by formation of an insoluble precipitate with cobalt chloride) on frozen brain sections as a measure of potential P85 toxicity in the BBB. There was no difference in ATPase activity in brain microvascular endothelial cells of control mice (Fig. 8C) or mice treated with P85 (Fig. 8F). The level of ATPase expression was assessed as the quantity of microvessels expressing ATPase. This was determined by image analysis (Fig. 8G) as the percent of area occupied by stained microvessels in gray and white matter that showed no statistically significant differences between control (untreated) and P85-treated groups ($p > 0.05$). These results indicate the absence of significant toxic effects of P85 *in vivo* at the doses used in these experiments.

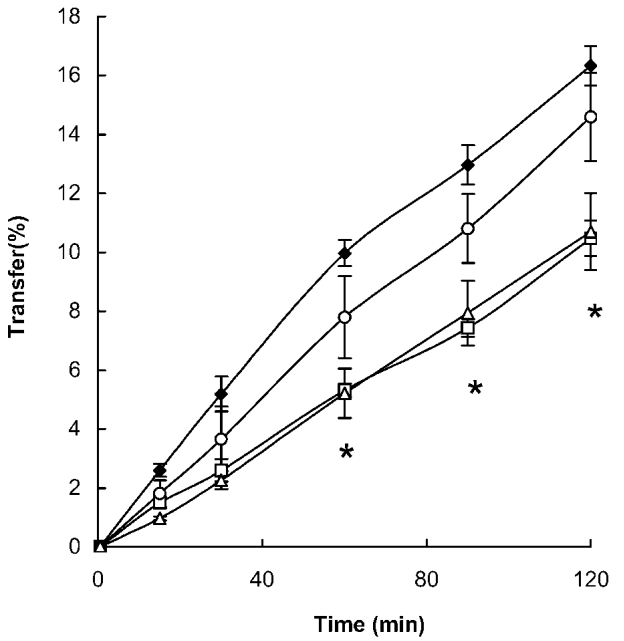

Fig. 7. Effect of P85 on ^{14}C-La flux in the BBMEC monolayers. Transport of the probe from luminal to abluminal side was examined in: assay buffer (filled diamonds); 0.01%wt P85 (open triangles); 0.1%wt P85 (open squares); or 1%wt P85 (open circles). Statistical significance of the P85 effects compared to the P85-free controls is shown on the figure: (*) $p < 0.05$; $n = 3$.

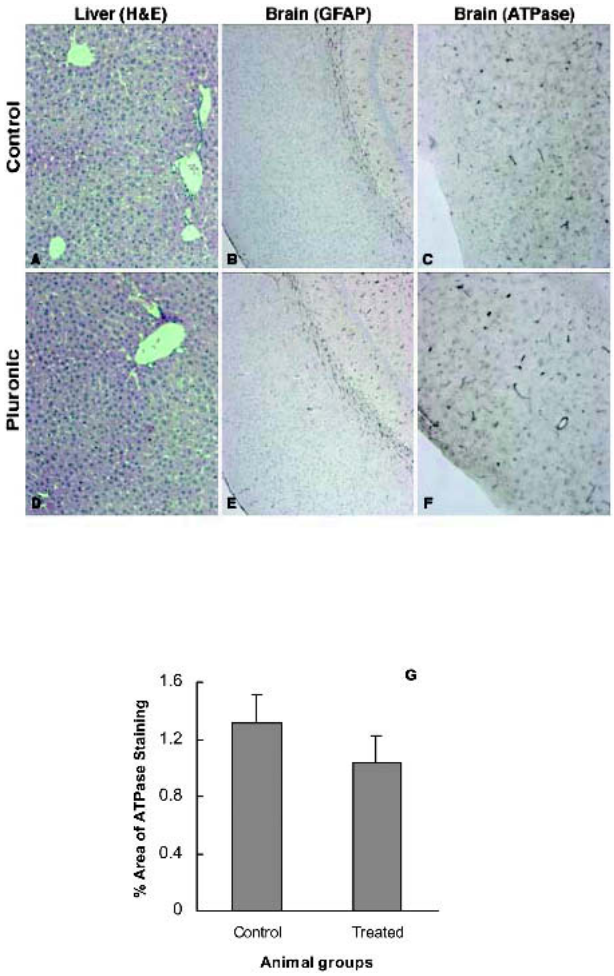

Fig. 8. Absence of significant P85 toxicity *in vivo*. Liver tissue from control (A) or treated animals (D) was free of significant histopathologic alterations. There was no increase in intensity of GFAP immunostaining in control (B) or P85-treated groups (E). Brain microvessels demonstrated similar ATPase activity in control (C) and treated animals (F) as confirmed by image analysis (G) expressed in percent of area occupied by stained microvessels in gray and white matter. Panels A and B, H&E; panels B and E, brain coronal sections immunostained with antibodies to GFAP and counterstained with Mayer's hematoxylin; panels C and F, ATPase *in situ* detection in brain coronal sections.

DISCUSSION

Pluronic block copolymers have attracted significant attention as chemosensitizing agents in chemotherapy due to their ability to inhibit the Pgp drug efflux transporter and thereby abolish mechanisms of drug resistance in cancer cells. Following the completion of phase I clinical trials a Pluronic formulation with doxorubicin is currently undergoing Phase II clinical trials for the treatment of the esophagus adenocarcinoma and soft tissue sarcoma, both cancers with high incidence of MDR. Recently, application of Pluronic formulations for CNS drug delivery was also suggested (10). We have demonstrated that Pluronic P85 can enhance the transport of a wide range of Pgp-dependent compounds, CNS drugs and imaging agents to the brain (11). However, along with advantages related to the increased permeability of the BBB, concern arises regarding possible side effects of Pluronics due to

the inhibition of other transport systems essential for normal brain function. In this paper, we have addressed the effects of Pluronics on the transport to the brain of major metabolic substrates, such as glucose and monocarboxylates. Although, GLUT1 and MCT1 transporters are not ATP-dependent, and therefore, intracellular ATP depletion caused by Pluronics may have no immediate effect on their function, they are membrane-associated proteins, which could be affected by Pluronic-induced alterations in cellular membranes. In particular, the hydrophobic PO chain of Pluronic block copolymer P85 used in this study is known to incorporate into the hydrophobic regions of cellular membranes resulting in their fluidization (19,20).

Based on the results of the accumulation and flux studies in BBMEC monolayers, we identified two opposite concentration-dependent effects of P85 on the GLUT1 transporter. Low doses of P85 (0.001 and 0.01% wt) appear to activate the transport function of GLUT1 resulting in slight increases in both, uptake and flux of the substrate. Conversely, high concentrations of P85 (0.1 and 1% wt) resulted in a decrease in 2-DG accumulation levels, although flux of the substrate was not altered. Because GLUT1 is expressed in both, luminal and abluminal membranes in BBMEC, as well as in the cytoplasm (21,22), we speculate that decreases in 2-DG accumulation at high P85 concentrations might be compensated by activation of GLUT1 in the cytoplasm and/or the abluminal membranes of the cells. In fact, compensatory mechanisms are well known for glucose transport in the BBB (23). Overall, P85 has minimal effect on the GLUT1-mediated flux and is unlikely to decrease the glucose supply to the brain.

The current study indicates that the effect of P85 on MCT1 transporter is complicated by the existence of efflux systems that we attribute to the expression of MRPs in brain microvessel endothelial cells (24). The fact that P85 has also been shown to affect MRPs makes picture even more convoluted. Because of this we were unable to use Michaelis-Menten analysis to quantify the P85 effects on MCT1. However, both accumulation and flux studies suggest that P85 can inhibit MCT1 in BBMEC. Interestingly, P85 has a maximal inhibition effect at concentrations 0.01–0.1% wt, which is in the vicinity of the critical micellar concentration (CMC) of the block copolymer. The same concentration dependency for the inhibitory effects of P85 has been reported for Pgp and MRPs transport systems (19,25), at concentrations of P85 that exceeded the CMC the inhibition effect was diminished. We relate these effects to lateral segregation of P85 in the membranes induced by the increasing concentration of the block copolymer (26). However, a possibility of some correlation between the effects of P85 on the Pgp and MRPs drug efflux transporters, and effects on GLUT1 and MCT1 cannot be excluded. A rationale for the lack of the P85 effects on glucose transport and inhibition of monocarboxylate transport in the BBB still need to be identified. One feature can make MCT1 more vulnerable for P85 than GLUT1, is its dependence on pH-gradient (27,28). Indeed, P85 was shown to inhibit efficiently H+-ATPase in the affected cells (29). This might be the Achilles heel of MCT1 for P85 inhibitory action. Overall, the results of the present study suggest that P85 might cause functional alterations in the monocarboxylate transporter that can interfere with the regulation of energy metabolism in the brain. Nevertheless, a careful histologic, immunohistochemical and enzyme histochemical examination showed no significant toxic effects of P85 multiple injections at the highest doses of the block copolymer used. This confirms safety of the P85 formulations for CNS drug delivery.

ACKNOWLEDGMENTS

This study was supported by National Institutes of Health grant NS36229. We are grateful to Peter Gwilt for helpful discussion and advice.

REFERENCES

1. T. S. Reese, N. Feder, and M. W. Brightman. Electron microscopic study of the blood-brain and blood-cerebrospinal fluid barriers with microperoxidase. *J. Neuropathol. Exp. Neurol.* **30**: 137–138 (1971).
2. A. M. Butt, H. C. Jones, and N. J. Abbott. Electrical resistance across the blood-brain barrier in anaesthetized rats: a developmental study. *J. Physiol.* **429**:47–62 (1990).
3. W. Pardridge. Introduction to the Blood–Brain Barrier. *Methodology, Biology and Pathology.* University Press: 486 (1998).
4. A. H. Schinkel, J. J. Smit, O. van Tellingen, J. H. Beijnen, E. Wagenaar, L. van Deemter, C. A. Mol, M. A. van der Valk, E. C. Robanus-Maandag and H. P. te Riele. Disruption of the mouse mdr1a P-glycoprotein gene leads to a deficiency in the blood-brain barrier and to increased sensitivity to drugs. *Cell* **77**:491–502 (1994).
5. K. A. Witt, J. D. Huber, R. D. Egleton, and T. P. Davis. Pluronic p85 block copolymer enhances opioid peptide analgesia. *J. Pharmacol. Exp. Ther.* **303**:760–767 (2002).
6. C. G. Lee, M. M. Gottesman, C. O. Cardarelli, M. Ramachandra, K. T. Jeang, S. V. Ambudkar, I. Pastan, and S. Dey. HIV-1 protease inhibitors are substrates for the MDR1 multidrug transporter. *Biochem.* **37**:3594–3601 (1998).
7. A. Tsuji and I. Tamai. Blood-brain barrier function of P-glycoprotein. *Adv. Drug Deliv. Rev.* **25**:287–298 (1997).
8. J. Weiss, C. J. Kerpen, H. Lindenmaier, S. M. Dormann, and W. E. Haefeli. Interaction of antiepileptic drugs with human P-glycoprotein in vitro. *J. Pharmacol. Exp. Ther.* **307**:262–267 (2003).
9. A. M. Karssen, O. C. Meijer, I. C. van der Sandt, A. G. De Boer, E. C. De Lange, and E. R. De Kloet. The role of the efflux transporter P-glycoprotein in brain penetration of prednisolone. *J. Endocrinol.* **175**:251–260 (2002).
10. A. V. Kabanov, E. V. Batrakova, and D. W. Miller. Pluronic block copolymers as modulators of drug efflux transporter activity in the blood-brain barrier. *Adv. Drug Deliv. Rev.* **55**:151–164 (2003).
11. E. Batrakova, S. Li, D. Miller, and A. Kabanov. Pluronic P85 increases permeability of a broad spectrum of drugs in polarized BBMEC and Caco-2 cell monolayers. *Pharm. Res.* **16**:1366–1372 (1999).
12. D. Miller, K. Audus, and R. Borchardt. Application of cultured bovine brain endothelial cells of the brain microvasiculature in the study of the blood-brain barrier. *J. Tissue Cult. Methods* **14**: 217–224 (1992).
13. E. Batrakova, S. Li, W. Elmquist, D. Miller, V. Alakhov, and A. Kabanov. Mechanism of sensitization of MDR cancer cells by Pluronic block copolymers: Selective energy depletion. *Br. J. Cancer* **85**:1987–1997 (2001).
14. E. Batrakova, D. Miller, S. Li, V. Alakhov, A. Kabanov, and W. Elmquist. Pluronic P85 enhances the delivery of digoxin to the brain: in vitro and in vivo studies. *J. Pharmacol. Exp. Ther.* **296**: 551–557 (2001).
15. P. K. Smith, R. I. Krohn, G. T. Hermanson, A. K. Mallia, F. H. Gartner, M. D. Provenzano, E. K. Fujimoto, N. M. Goeke, B. J. Olson, and D. C. Klenk. Measurement of protein using bicinchoninic acid. *Anal. Biochem.* **150**:76–85 (1985).
16. D. Bylund and L. Murrin. Radioligand saturation binding experiments over large concentration ranges. *Life Sci.* **67**:2897–2911 (2000).
17. D. B. Bylund. Graphic presentation and analysis of inhibition

data from ligand-binding experiments. *Anal. Biochem.* **159**:50–57 (1986).
18. W. E. Zink, E. Anderson, J. Boyle, L. Hock, J. Rodriguez-Sierra, H. Xiong, H. E. Gendelman, and Y. Persidsky. Impaired spatial cognition and synaptic potentiation in a murine model of human immunodeficiency virus type 1 encephalitis. *J. Neurosci.* **22**:2096–2105 (2002).
19. E. Batrakova, S. Li, S. Vinogradov, V. Alakhov, D. Miller, and A. Kabanov. Mechanism of pluronic effect on P-glycoprotein efflux system in blood-brain barrier: contributions of energy depletion and membrane fluidization. *J. Pharmacol. Exp. Ther.* **299**:483–493 (2001).
20. E. Batrakova, S. Li, V. Alakhov, D. Miller, and A. Kabanov. Optimal structure requirements for pluronic block copolymers in modifying P-glycoprotein drug efflux transporter activity in bovine brain microvessel endothelial cells. *J. Pharmacol. Exp. Ther.* **304**:845–854 (2003).
21. I. A. Simpson, S. J. Vannucci, M. R. DeJoseph, and R. A. Hawkins. Glucose transporter asymmetries in the bovine blood-brain barrier. *J. Biol. Chem.* **276**:12725–12729 (2001).
22. W. M. Pardridge, R. J. Boado, and C. R. Farrell. Brain-type glucose transporter (GLUT-1) is selectively localized to the blood-brain barrier. Studies with quantitative western blotting and in situ hybridization. *J. Biol. Chem.* **265**:18035–18040 (1990).
23. C. G. Gaposchkin and J. F. Garcia-Diaz. Modulation of cultured brain, adrenal, and aortic endothelial cell glucose transport. *Biochim. Biophys. Acta* **1285**:255–266 (1996).
24. Y. Zhang, H. Han, W. F. Elmquist, and D. W. Miller. Expression of various multidrug resistance-associated protein (MRP) homologues in brain microvessel endothelial cells. *Brain Res.* **876**:148–153 (2000).
25. E. V. Batrakova, S. Li, V. Y. Alakhov, W. F. Elmquist, D. W. Miller, and A. V. Kabanov. Sensitization of cells overexpressing multidrug-resistant proteins by pluronic P85. *Pharm. Res.* **20**:1581–1590 (2003).
26. K. Kostarelos, T. Tadros, and P. Luckham. Physical conjugation of (Tri-) block copolymers to liposomes toward the concentration of sterically stabilized vesicle systems. *Langmuir* **15**:369–376 (1999).
27. R. C. Poole and A. P. Halestrap. Transport of lactate and other monocarboxylates across mammalian plasma membranes. *Am. J. Physiol.* **264**:C761–C782 (1993).
28. C. Juel. Lactate-proton cotransport in skeletal muscle. *Physiol. Rev.* **77**:321–358 (1997).
29. V. Alakhov, E. Klinski, S. Li, G. Pietrzynski, A. Venne, E. V. Batrakova, T. Bronitch, and A. Kabanov. Block copolymer-based formulation of Doxorubicin. From cell screen to clinical trials. *Colloids Surf. B Biointerfaces* **16**:113–134 (1999).